

NUMERICAL INVESTIGATION OF THREE-PHASE FLOWS USING INCOMPRESSIBLE SMOOTHED PARTICLE HYDRODYNAMICS

Amir Zainali[†], Nima Tofghi[†] and Mehmet Yildiz[†]

[†]Faculty of Engineering and Natural Sciences,
Advanced Composites and Polymer Processing Laboratory,
Sabanci University, Orhanli 34956, Tuzla, Istanbul, Turkey
e-mail: meyildiz@sabanciuniv.edu,
<http://people.sabanciuniv.edu/meyildiz/>

Key words: SPH, multiphase flows, meshfree, phase specific surface tension

Abstract. An ISPH method for the simulation of three-phase flows is presented in this article. The proposed method is investigated through the simulation of a droplet located at the interface of two immiscible fluids as well as diamond droplet deformation. The extendibility of the proposed surface tension formulations for three-phase flows to two-phase flows is also investigated. It is observed that the results obtained from the numerical simulations are in good agreement with the analytical ones.

1 Introduction

Two-phase flows are investigated extensively numerically in the literature during the past decades while the physics behind the three and more phase flow problems are relatively unknown despite the fact that Multi-phase flows play an important role in many industrial and physical phenomena. Typical examples with many applications in chemical and biomedical industries include mixture of three or more fluids (e.g. oil-water-gas mixture in oil industry) and compound droplets. The main reason for the scarcity of numerical simulations for three-phase flows in comparison to two-phase flows can be due to the complications associated with the modeling of hydrodynamical interactions at the interface for three-component systems [3, 4, 6].

In this work, we have developed a 2-D multiphase incompressible smoothed particle hydrodynamics (ISPH) model based on the standard projection method initially used by Cummins and Rudman [2] for SPH, while the continuum surface force model proposed by Brackbill et al. [1] is used to model surface tension forces. The method proposed by Smith et al. [6] is implemented to take into account different surface tension coefficients between the phases in a three-component system.

This paper is organized as follows. In section 2, the mathematical formulations as well as numerical scheme are briefly described. In section 3, numerical results are presented. Finally in section 4 concluding remarks are provided.

2 Governing Equations

All constituents of the multiphase system are considered to be viscous, Newtonian and incompressible liquids with constant material properties, $D\Gamma/Dt = 0$, where $D/Dt = \partial/\partial t + (\cdot)_{,k} v_k$ is the material time derivative operator. The set of equations governing the motion of the flow under consideration are conservation of mass and linear momentum. In their local form for volume and discontinuity surface, these equations may be specified as

$$D\rho/Dt = -\rho v_{k,k}, \quad \text{on } V-\sigma \quad (1)$$

$$\rho Dv_l/Dt = \tau_{kl,k} - \rho b_l, \quad \text{on } V-\sigma \quad (2)$$

$$\|\rho(v_k - u_k)\| \hat{n}_k = 0, \quad \text{on } \sigma \quad (3)$$

$$\|\rho v_l(v_k - u_k) - \tau_{kl}\| \hat{n}_k = f_l^\sigma, \quad \text{on } \sigma \quad (4)$$

where $V-\sigma$ denotes total volume, excluding the points lying on the surface of discontinuity, σ . Equations (1) and (2) are valid within the body excluding σ while equations (3) and (4) are valid only on the surface of discontinuity and represent the jump condition across σ . $\tau_{kl} = -p\delta_{kl} + 2\mu d_{kl}$ is the symmetric total stress tensor, $d_{kl} = 0.5(v_{k,l} + v_{l,k})$ is the symmetric deformation tensor, δ_{kl} is the Kronecker delta, p is the thermodynamic pressure, b_l is the body force, f_l^σ is the surface force per unit area on the interface due to surface tension for the mixture, v_k is the divergence-free velocity, ρ and μ are the density and viscosity of the mixture. The symbol $\|\phi\|$ indicates the jump of the enclosed quantity across the discontinuity surface, $\phi^+ - \phi^-$ where ϕ^+ and ϕ^- are the values of ϕ on the positive and the negative sides of the discontinuity surface. Here, u_k denotes the velocity of the discontinuity surface, \hat{n}_k is the unit normal to the discontinuity surface.

One can write the local form of the jump condition for the momentum balance as

$$f_l^\sigma = \|p\| n_l = \gamma\kappa\hat{n}_l \quad (5)$$

where surface tension coefficient, γ , is assumed to be constant. Here, $\kappa = -n_{m,m}$ is the curvature. For the sake of computational efficiency and simplification, it is preferable to express local surface force as an equivalent volumetric force (the force per unit volume). This can be achieved by using the continuum surface force model (CSF) proposed in [1]. Using this approach equation (5) can be expressed as a volume force by multiplying the local surface tension force with a one-dimensional delta function defined on the interface, δ ,

$$f_l^{\sigma v} = \sigma\kappa\hat{n}_l\delta \quad (6)$$

In this study, to track the interface each particle is assigned to a color function,

$$C_{\mathbf{i}}^{\alpha} = \begin{cases} 1, & \text{if } \mathbf{i} \text{ belongs to fluid } \alpha \\ 0, & \text{else} \end{cases} \quad (7)$$

and finally, 1-D delta function on the interface is chosen to be $\delta = |C_{,m}|$.

In the treatment of multiphase immiscible fluids with two constituents, the implementation of the continuum surface force model is straightforward in that there is only one interface between the constituents. On the other hand, in the multiphase systems with more than two constituents, an interface fluid particle may see two or more interfaces at the same time and in what follows a decision should be made as to which surface tension coefficient is to be used. To be able resolve this difficulty, in [6] the surface tension coefficient was decomposed into phase specific surface tension such that $\gamma^{\alpha\beta} = \gamma^{\alpha} + \gamma^{\beta}$ where $\gamma^{\alpha\beta}$ is the physical surface tension coefficient between the phase α and the phase β , and γ^{α} and γ^{β} are the phase specific surface tension coefficients for α^{th} and β^{th} phases respectively. For three-phase system, $\gamma^{12} = \gamma^1 + \gamma^2$, $\gamma^{13} = \gamma^1 + \gamma^3$, and $\gamma^{23} = \gamma^2 + \gamma^3$. Upon solving a linear system of equations for γ^1 , γ^2 and γ^3 , one can write the following relations among the physical and phase specific surface tension coefficients as $\gamma^1 = 0.5(\gamma^{12} + \gamma^{13} - \gamma^{23})$, $\gamma^2 = 0.5(\gamma^{12} - \gamma^{13} + \gamma^{23})$, and $\gamma^3 = 0.5(-\gamma^{12} + \gamma^{13} + \gamma^{23})$. As such, for each particle, three phase specific normals, curvatures, and the surface tension forces are computed. The total surface tension force acting on the given interface particle is then the sum of three phase specific surface tension forces such that $f_{il}^{\sigma v} = \sum_{\alpha=1}^3 f_{il}^{(\sigma v)\alpha}$ where the subscript \mathbf{i} is a particle identifier, and the adjacent Latin letter is the l^{th} component of the surface force.

2.1 SPH preliminaries and the numerical method

The numerical method used in this work for linearizing the governing equations and associated interface and boundary conditions is based on the Incompressible Smoothed Particle Hydrodynamics method presented in [5], which is briefly described in what follows.

SPH particles interact with each other by means of an interpolation (weighting, smoothing, kernel) function $W(r_{\mathbf{ij}}, h)$, concisely designated as $W_{\mathbf{ij}}$ for a constant h . Here, $r_{\mathbf{ij}}$ is the magnitude of the distance vector $\vec{r}_{\mathbf{ij}} = \vec{r}_{\mathbf{i}} - \vec{r}_{\mathbf{j}}$ between the particle of interest \mathbf{i} and its neighboring particles \mathbf{j} , and h is referred to as the smoothing length which controls the interaction length among particles.

In the SPH method, an arbitrary function (i.e, scalar $f(\vec{r}_{\mathbf{i}})$, vectorial $f^p(\vec{r}_{\mathbf{i}})$, or tensorial $f^{ps}(\vec{r}_{\mathbf{i}})$) may be approximated as $f_{\mathbf{i}}^p = \int_{\Omega} f_{\mathbf{j}}^p W_{\mathbf{ij}} d^3\vec{r}_{\mathbf{j}}$ where $f^p(\vec{r}_{\mathbf{i}})$ is briefly denoted by $f_{\mathbf{i}}^p$. Upon replacing the integral operation with a summation sign over all the particles within the cut-off distance (i.e. $r_{\mathbf{ij}} < Kh$, where K is a constant coefficient for the selected kernel function), and approximating the infinitesimal volume element by reciprocal of the number density $\psi_{\mathbf{j}}$, defined for the particle \mathbf{j} , one can write the SPH approximation of $f_{\mathbf{i}}^p$

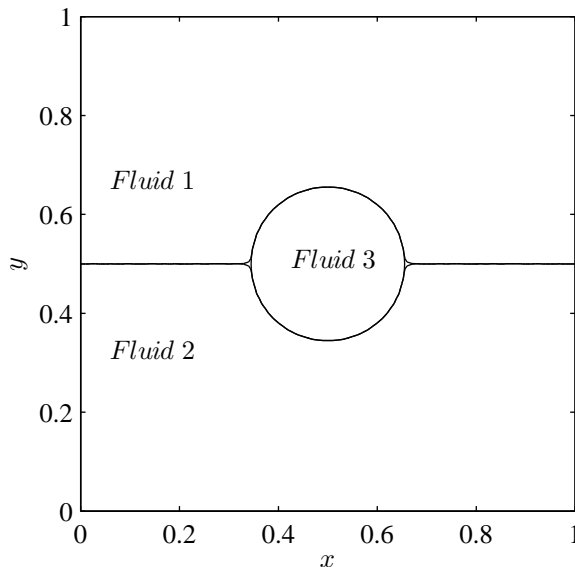


Figure 1: Domain size and fluid numbers at the initial condition for different simulations (The bubble has a diameter of 0.3 with its center coordinates at 0.5, and 0.5.)

as

$$f_{\mathbf{i}}^p = f^p(\mathbf{r}_{\mathbf{i}}) = \sum_{\mathbf{j}} \frac{1}{\psi_{\mathbf{j}}} f_{\mathbf{j}}^p W_{\mathbf{ij}} \quad (8)$$

where the number density for particle \mathbf{i} is defined as $\psi_{\mathbf{i}} = \sum_{\mathbf{j}} W_{\mathbf{ij}}$

Upon using a differentiable smoothing function, the spatial first order derivative of the function $f_{\mathbf{i}}^p$ evaluated at the location of particle \mathbf{i} can simply be approximated through multiplying the gradient of the kernel function $\partial W_{\mathbf{ij}}/\partial x_{\mathbf{i}}^s$ (taken with respect to the particle \mathbf{i}) by the field variables and volumes of neighbor particles. There are several ways to discretize the first order spatial derivative of a field variable. Throughout this work, the one used is of the following form

$$\frac{\partial f_{\mathbf{i}}^p}{\partial x_{\mathbf{i}}^k} a_{\mathbf{ij}}^{ks} = \sum_{\mathbf{j}} \frac{1}{\psi_{\mathbf{j}}} (f_{\mathbf{j}}^p - f_{\mathbf{i}}^p) \frac{\partial W_{\mathbf{ij}}}{\partial x_{\mathbf{i}}^s} \quad (9)$$

where $a_{\mathbf{ij}}^{ks}$ is a corrective second-rank tensor given by,

$$a_{\mathbf{ij}}^{ks} = \sum_{\mathbf{j}} \frac{r_{\mathbf{ij}}^k}{\psi_{\mathbf{j}}} \frac{\partial W_{\mathbf{ij}}}{\partial x_{\mathbf{i}}^s} \quad (10)$$

This form is referred to as the corrective SPH gradient formulation that can be used to eliminate particle inconsistencies. It should be noted that the corrective term $a_{\mathbf{ij}}^{ks}$ is ideally equal to Kronecker delta, δ^{ks} for a continuous function. As for SPH approximation to

the second order derivative of a vector-valued function, it can be written in two different ways as

$$\frac{\partial^2 f_{\mathbf{i}}^p}{\partial x_{\mathbf{i}}^k \partial x_{\mathbf{i}}^k} a_{\mathbf{ij}}^{pm} = 8 \sum_{\mathbf{j}} (f_{\mathbf{i}}^p - f_{\mathbf{j}}^p) \frac{r_{\mathbf{ij}}^p}{r_{\mathbf{ij}}^2} \frac{\partial W_{\mathbf{ij}}}{\partial x_{\mathbf{i}}^m}, \quad (11)$$

$$\frac{\partial^2 f_{\mathbf{i}}^p}{\partial x_{\mathbf{i}}^k \partial x_{\mathbf{i}}^k} (2 + a_{\mathbf{ij}}^{ss}) = 8 \sum_{\mathbf{j}} (f_{\mathbf{i}}^p - f_{\mathbf{j}}^p) \frac{r_{\mathbf{ij}}^s}{r_{\mathbf{ij}}^2} \frac{\partial W_{\mathbf{ij}}}{\partial x_{\mathbf{i}}^s}. \quad (12)$$

For the time integration in the ISPH approach, two-stage predictor-corrector method with a first-order Euler time step scheme is used. The algorithm starts with the predictor step where the intermediate positions $\vec{r}_{\mathbf{i}}^*$ for all particles are calculated through the knowledge of preceding particle positions $\vec{r}_{\mathbf{i}}^{(n)}$ and the previous correct velocity field $\vec{v}_{\mathbf{i}}^{(n)}$ as $\vec{r}_{\mathbf{i}}^* = \vec{r}_{\mathbf{i}}^{(n)} + \vec{v}_{\mathbf{i}}^{(n)} \Delta t$. The intermediate velocity field $\vec{v}_{\mathbf{i}}^*$ is calculated on the intermediate particle locations by solving the momentum balance equations with forward time integration without the pressure gradient term as $\vec{v}_{\mathbf{i}}^* = \vec{v}_{\mathbf{i}}^{(n)} + \vec{f}_{\mathbf{i}}^{(n)} \Delta t$. The pressure Poisson equation is solved to obtain the pressure, $p_{\mathbf{i}}^{(n+1)}$, which is required to enforce the incompressibility condition. The actual velocity field at time step $(n+1)$, $\vec{v}_{\mathbf{i}}^{(n+1)}$, can be obtained by using the computed pressure. Finally, with the correct velocity field for time-step $(n+1)$, all fluid particles are moved to their new positions $\vec{r}_{\mathbf{i}}^{(n+1)} = \vec{r}_{\mathbf{i}}^{(n)} + 0.5 \left(\vec{v}_{\mathbf{i}}^{(n)} + \vec{v}_{\mathbf{i}}^{(n+1)} \right) \Delta t$.

3 Results and Discussion

In this section, results of the conducted simulations are presented. Computational domain for every simulation is taken to be a square with the side length of 1. Each row and column consists of 100 equally spaced particles for test cases evolving from a Cartesian particle arrangement. Test cases with non-Cartesian particle arrangement have the same number of particles as with their Cartesian counterparts. All fluid properties are set to unity for every phase involved in simulations while binary surface tension coefficient assumes a value of 0 or 1, depending on the test cases considered. Different phases are ordered as shown in figure 1. No-slip boundary conditions for the top and bottom, and side walls are applied. Zero pressure boundary condition is applied for all boundaries.

In order to test the applicability of the three-phase surface tension treatment to two-phase flow systems, the deformation of the initially diamond-shaped droplet under the effect of the surface tension force is considered. Particles of fluid 3 are initially positioned on a diamond surrounded by fluid 1 and 2 particles. The binary surface tension coefficient between fluids 1 and 2 is set to zero so as to make them act like a single fluid. Figure 2 provides the sequences of shape-evolution of the diamond bubble in the aforementioned test case in detail. The initial diamond evolves in time hence becoming a circle as the simulation continues. The circle obtained in this way is also used for the initial positioning of particles in some other test cases. As expected, the new surface tension treatment method presented for SPH of three-phase fluid flow is also applicable to a two-phase fluid

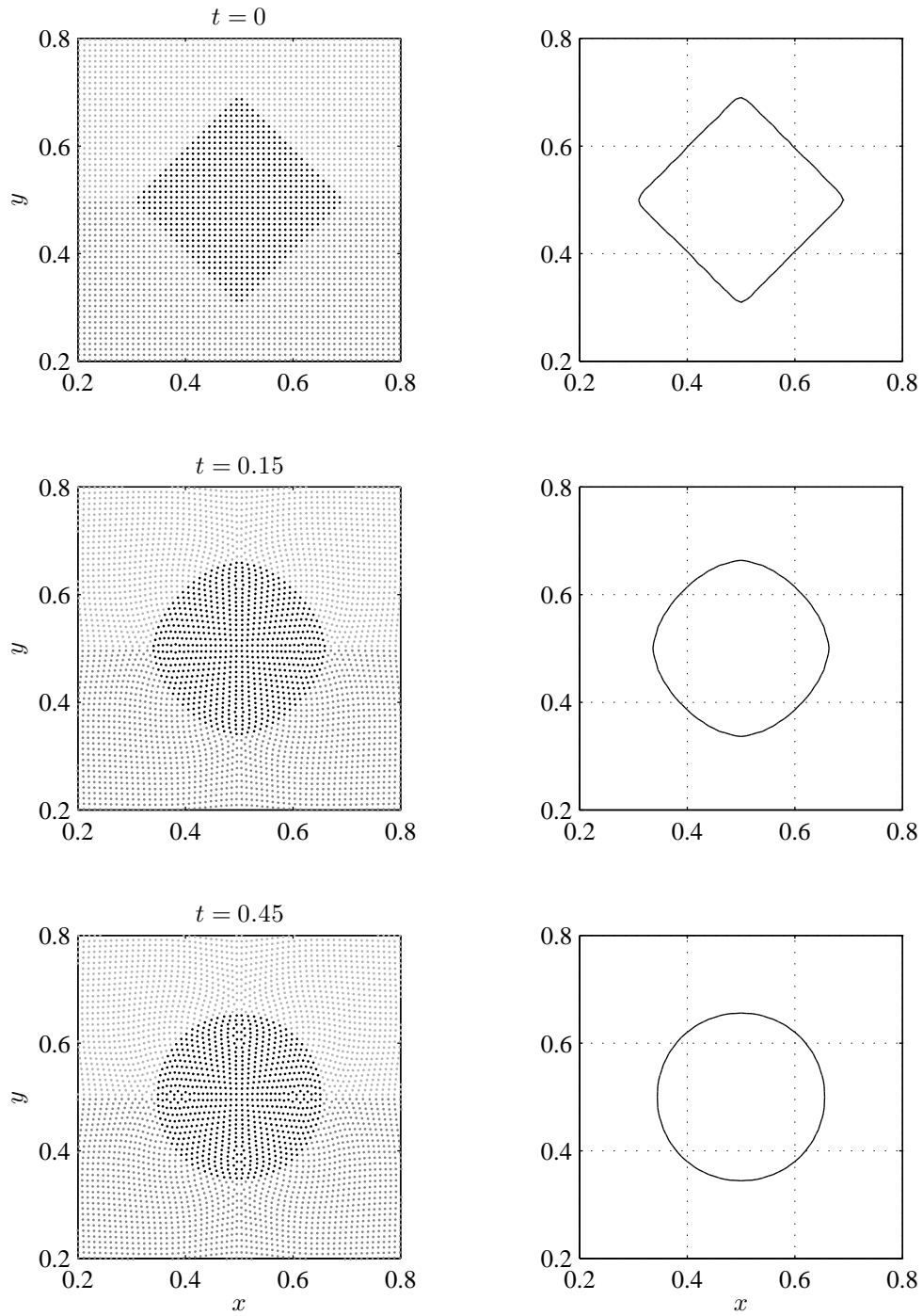


Figure 2: The time evolution of a diamond shaped bubble to a circle shape bubble; Left: particle positions, Right: color contour showing bubble boundary.

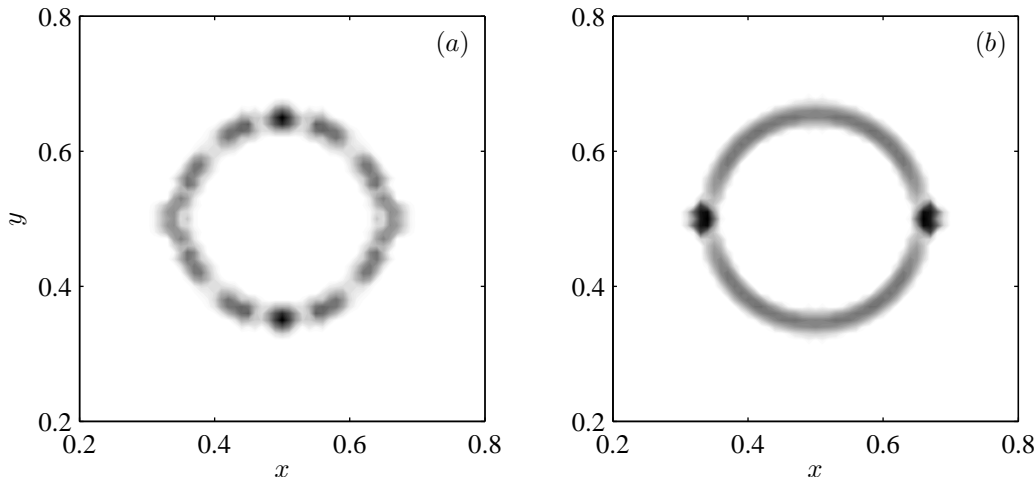


Figure 3: Contours of surface tension force magnitude for different initial particle positioning at $t = 0.015$ s; (a) crude circle marked in cartesian distribution, (b) circle obtained from evolution of a diamond.

system.

In this study, two different methods are used for the initial arrangement of particles in a circular bubble positioned in a rectangular domain for the liquid lens. In the first method, all the particles are placed on a Cartesian grid and the bubble is formed through assigning different phases to each particle in accordance with their positions. The circular bubble obtained by this method is rather crude thereby presenting many irregularities in shape which eventually result in an intermittent surface tension force as shown in figure 3-a. In the second method, an initial diamond shaped bubble is allowed to deform into a circular bubble in a two phase flow as described previously. The simulation using an initial circular bubble generated by the second method leads to improvements in the surface tension force and particle positions, as seen in figure 3-b. The initial diameter for the crude bubble used here is 0.293 while the bubble obtained from the diamond shape has a diameter of 0.299. The reason behind this difference is that it is almost impossible to create a circular bubble shape of desired initial diameter (in this work, the initial diameter of interest is 0.3) from limited number of equally spaced particles on a Cartesian grid. The crude circle experiences an abrupt change in particle positions at early stages of the simulation due to the aforementioned irregular surface tension force. This affects the initial reading for the diameter, rendering it difficult to compare the results with analytical data. This problem is more evident in figure 4-a, where lens diameter versus time is shown for both test cases. While both test cases show the same characteristics, the crude bubble has smaller elongation rate along the major axis. The results are more evident when the transverse diameter of the lens is normalized by the analytically obtained equilibrium diameter, as shown in 4-b.

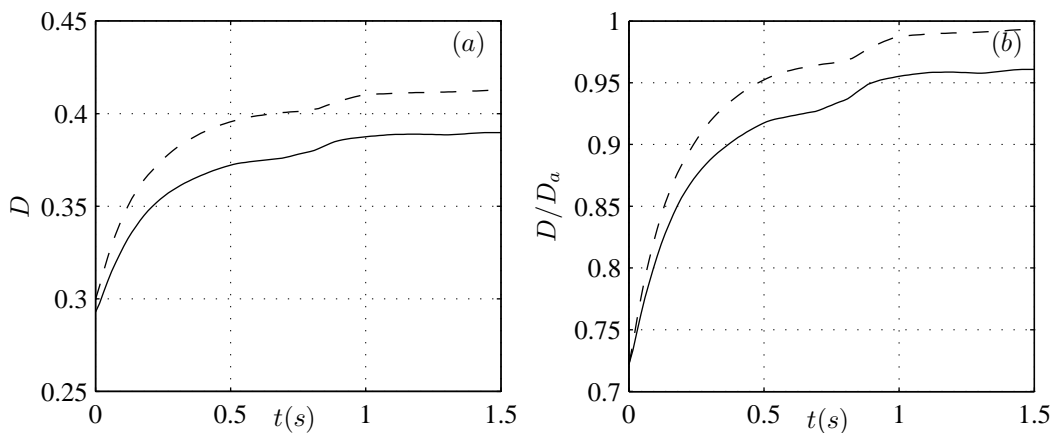


Figure 4: Change in transverse lens diameter versus time for different initial conditions; Solid line: crude circle marked in Cartesian distribution, Dashed line: circle obtained from evolution of a diamond.

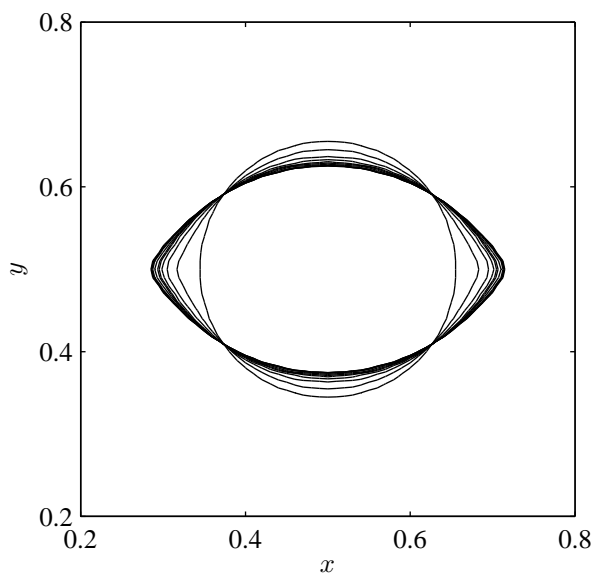


Figure 5: The time evolution of the liquid lens visualized by color contours.

The shape of the droplet is controlled by the values of the surface tension forces. Therefore, under the effect of these surface tension forces, the initially circular droplet deforms into an elliptic or lens shape. The equilibrium three-phase contact angle is formulated as $\sin \varphi_1/\gamma_{23} = \sin \varphi_2/\gamma_{13} = \sin \varphi_3/\gamma_{12}$. The transverse diameter of the lens along the major axis (the distance between triple junctions) is computed through [4]

$$d = \left(\frac{2(\pi - \varphi_1) - \sin(2\pi - 2\varphi_1)}{8A \sin^2(\pi - \varphi_1)} + \frac{2(\pi - \varphi_3) - \sin(2\pi - 2\varphi_3)}{8A \sin^2(\pi - \varphi_3)} \right) \quad (13)$$

where φ_α is the contact angle of the α^{th} phase, and A is the area of the liquid lens.

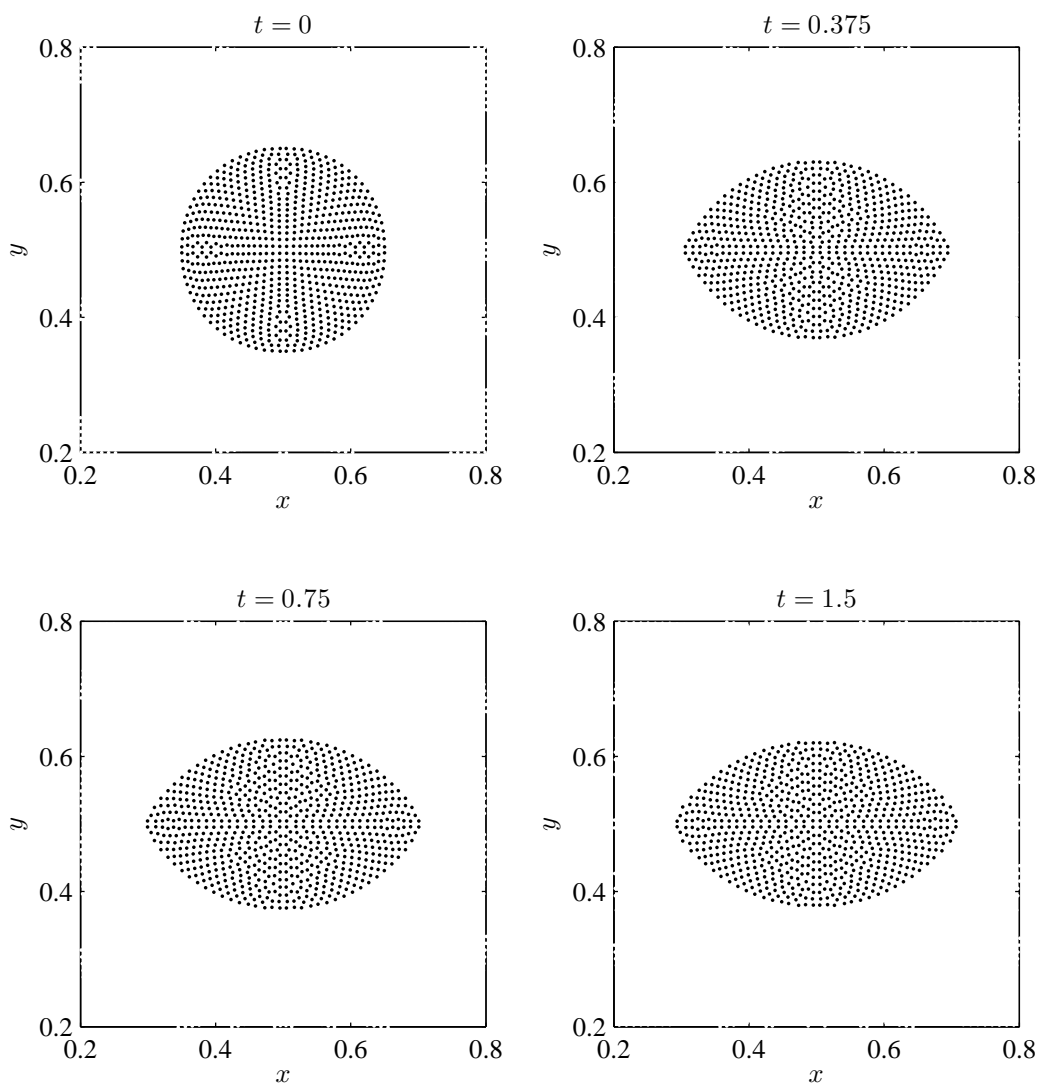


Figure 6: Particle positions for liquid lens at different simulation times.

Based on the initial diameter of circle obtained from a diamond, equation (13) predicts a diameter of 0.415 while the result obtained from the simulation is 0.413. It is obvious in figure 4-a that the difference between theory and simulation is much greater in the case where a crude circle is used as the initial condition for the simulations. The analytical result for the crude circle is 0.406 and the simulation results in an equilibrium diameter of 0.389. It is obvious in figure 4-b that the difference between theory and simulation is much greater in the case where a crude circle is used as the initial condition for the

simulations.

Having chosen the second method for generating an initial circular bubble geometry, figure 5 shows the time evolution of a fluid lens between two layers of fluid. In this case, all fluid properties are set to 1 while binary surface tension coefficients, γ_{ij} , are equal between each pair of surfaces. The time snapshots for particle positions inside the lens is also provided in figure 6.

4 Conclusions

In this study, a three-phase ISPH method is developed and presented for the simulation of the three-phase flows. Phase specific surface tension coefficient [6] is used to obtain the surface tension force for the systems with three components. The applicability of this formulations for two-phase flows is demonstrated. In addition, It is observed that choosing appropriate initial condition is crucial to obtain accurate results. And finally, it is shown that the equilibrium three-phase transverse lens diameter obtained is in good agreement with the analytical one.

5 Acknowledgement

Funding provided by the European Commission Research Directorate General under Marie Curie International Reintegration Grant program with the Grant Agreement number of PIRG03- GA-2008-231048 is gratefully acknowledged.

References

- [1] J. U. Brackbill, D. B. Kothe, and C. Zemach. A continuum method for modeling surface tension* 1. *Journal of computational physics*, 100(2):335–354, 1992.
- [2] S. J. Cummins and M. Rudman. An sph projection method. *Journal of computational physics*, 152(2):584–607, 1999.
- [3] J. Kim. Phase field computations for ternary fluid flows. *Computer methods in applied mechanics and engineering*, 196(45-48):4779–4788, 2007.
- [4] J. S. Kim and J. Lowengrub. Phase field modeling and simulation of three-phase flows. *Interfaces and free boundaries*, 7(4):435, 2005.
- [5] M. S. Shadloo, A. Zainali, S. H. Sadek, and M. Yildiz. Improved incompressible smoothed particle hydrodynamics method for simulating flow around bluff bodies. *Computer methods in applied mechanics and engineering*, 200(9-12):1008–1020, 2011.
- [6] K. A. Smith, F. J. Souls, and D. L. Chopp. A projection method for motion of triple junctions by level sets. *Interfaces and free boundaries*, 4(3):263–276, 2002.